Electrical performance verification methodology for large reflector antennas: based on the P-band SAR payload of the ESA BIOMASS candidate mission

Pivnenko, Sergey; Kim, Oleksiy S.; Nielsen, Jeppe Majlund; Breinbjerg, Olav; Pontoppidan, K.; Østergaard, A.; Lin, C. C.

Published in:
C E A S Space Journal

Link to article, DOI:
10.1007/s12567-013-0040-y

Publication date:
2013

CEAS Space J
DOI 10.1007/s12567-013-0040-y

ORIGINAL PAPER

Electrical performance verification methodology for large reflector antennas: based on the P-band SAR payload of the ESA BIOMASS candidate mission

S. Pivnenko · O. S. Kim · J. M. Nielsen · O. Breinbjerg · K. Pontoppidan · A. Østergaard · C. C. Lin

Received: 25 January 2013 / Revised: 5 June 2013 / Accepted: 7 June 2013

Abstract In this paper, an electrical performance verification methodology for large reflector antennas is proposed. The verification methodology was developed for the BIOMASS P-band (435 MHz) synthetic aperture radar (SAR), but can be applied to other large deployable or fixed reflector antennas for which the verification of the entire antenna or payload is impossible. The two-step methodology is based on accurate measurement of the feed structure characteristics, such as complex radiation pattern and radiation efficiency, with an appropriate measurement technique, and then accurate calculation of the radiation pattern and gain of the entire antenna including support and satellite structure with an appropriate computational software. A preliminary investigation of the proposed methodology was carried out by performing extensive simulations of different verification approaches. The experimental validation of the methodology included measurements of the prototype BIOMASS feed in several structural configurations with spherical, cylindrical, and planar near-field techniques. The measured characteristics for the feed structure were then used in the calculation of the radiation pattern and gain of the entire reflector antenna. The main emphasis of the work was on the assessment of the achievable pattern and gain uncertainty for the entire antenna and its compliance with the BIOMASS SAR requirements.

Keywords Electrical performance verification · On-ground payload verification · Deployable reflector antenna · Antenna measurement · Measurement uncertainty

1 Introduction

Large reflector antennas are extensively used in various applications such as Earth Observation radars and radiometers, radio astronomy, communication systems, data relay satellites, etc. In many of these applications, the reflectors are very large, either mechanically or electrically, or both, thus presenting many challenges regarding their accurate design, manufacturing, and verification [1]. An accurate electrical verification of large reflector antennas may represent an extremely difficult task, for example, deployable reflectors intended for space application may only be designed to operate in zero gravity or their size is beyond the capability of available measurement facilities. Their on-ground verification may thus not be possible or is associated with extreme technical challenges.

One such example is the BIOMASS candidate mission currently undergoing its feasibility phase in the selection process for the seventh Earth Explorer cycle of the European Space Agency (ESA) [2]. The aim of the BIOMASS mission is to determine the distribution and track the temporal changes of forest biomass at a global scale. This

This paper is based on a presentation at the ESA Workshop on Large Deployable Antennas, October 2–3, 2012, Noordwijk, The Netherlands.

S. Pivnenko (✉) · O. S. Kim · J. M. Nielsen · O. Breinbjerg
Technical University of Denmark, Ørsteds Plads, 348,
2800 Kongens Lyngby, Denmark
e-mail: sp@elektro.dtu.dk

K. Pontoppidan
TICRA, Læderstræde 34, 1201 Copenhagen, Denmark
e-mail: kp@ticra.com

A. Østergaard · C. C. Lin
ESA-ESTEC, Keplerlaan 1, 2200 AG Noordwijk,
The Netherlands
e-mail: allan.ostergaard@esa.int

Published online: 02 July 2013

is important information as those biomass parameters are related to the amount of carbon dioxide absorbed from and released to the atmosphere. Data from the BIOMASS mission will contribute to the understanding of the carbon cycle and its role in controlling the climate [2].

The main payload of the BIOMASS is a P-band (435 MHz) synthetic aperture RADAR (SAR) with an antenna aperture of approximately 110 m^2 with full polarimetric and multi-pass interferometric capabilities [3]. The baseline antenna configuration is a large deployable reflector antenna illuminated by a small patch-antenna feed array. The reflector consists of a deployable support structure holding a wire mesh shaped to a parabolic reflecting surface. It has a projected aperture with a diameter of 11.5 m and a focal length of 7.5 m and it is held by a foldable arm at a proper distance and orientation with respect to the satellite. The dual-polarized feed is a 2 × 2 patch array of about 1 m^2 located on the top shelf of the satellite having dimensions of about 1 × 1.5 × 3 m^3 (see illustration in Fig. 1). The feed and the reflector are folded towards the satellite during the launch and deployed in orbit.

The absolute radiometric accuracy of the entire P-band instrument, including errors from propagation, processing and calibration, is required to be better than 1 dB (1σ). Since the antenna pattern enters the total SAR uncertainty budget twice, the accurate knowledge of in-flight performance of the antenna pattern and gain becomes essential. The one-way gain accuracy for the SAR antenna is required to be better than 0.15 dB (1σ), which is a very challenging value for any measurement considering the low operation frequency, dimensions, and geometry of the satellite and the reflector, as well as influence of the gravity force on the deployable mesh reflector during the on-ground SAR verification.

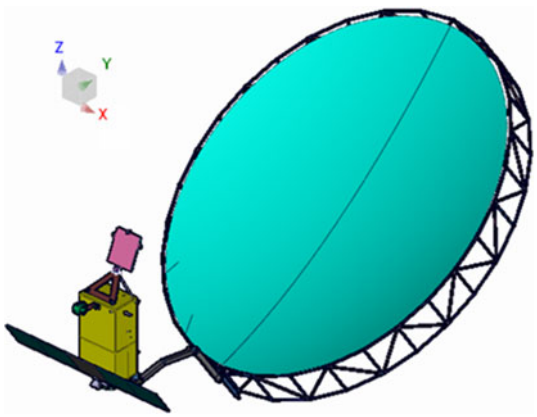

Fig. 1 One of the possible BIOMASS satellite configurations with the deployable reflector antenna (courtesy of Thales Alenia Space, Italy). The large deployed reflector (*blue*) is illuminated by the square feed antenna (*purple*) sitting on its triangular support structure (*brown*) on top of the box-shaped satellite (*green*) holding also a deployed rectangular solar panel (*brown*)

2 Review of verification approaches

In order to overcome the technical challenges associated with the on-ground electrical performance verification of large deployable and fixed reflector antennas, various approaches were proposed over the years. Several potential approaches applicable for the BIOMASS antenna were reviewed and analyzed in [4, 5].

The first approach is the measurement of the entire SAR antenna in the final deployed configuration. In this approach, the SAR antenna is deployed in a suitable anechoic chamber and its RF characteristics are measured with an appropriate near-field technique (see description of the near-field techniques in Sect. 5). The advantage of such an approach is that the entire antenna is validated in one run. This approach, however, faces a series of severe practical problems:

- The deployment mechanisms are often designed to work in zero-gravity conditions and thus deployment in the gravity force may not be possible. Usual gravity compensation approaches may not be directly applicable to this configuration and may not be compatible with the measurement technique.
- The gravity force affects the shape of the mesh deforming the reflecting surface to a non-correct shape. Potentially, various gravity compensation approaches can be used to correct the surface shape to be within the required accuracy, but again they may not be compatible with the measurement technique.
- The RF measurement of the deployed reflector of the considered size with the satellite, which is about 12 × 18 × 10 m altogether in an upwards looking orientation, requires a shielded anechoic chamber of at least twice the size in each dimension and operating at 435 MHz.
- The RF measurement of the deployed reflector with, e.g. a planar near-field (PNF) technique would require the scan zone area of about 20 × 30 m for the ± 45° valid angular region.

In view of the listed practical issues, the measurement of the entire reflector is extremely challenging and thus not the preferred approach.

The second approach is the measurement of a scaled model. In this approach, a down-scaled model of the reflector antenna, the feed, and the satellite are manufactured and measurements are performed at the correspondingly up-scaled frequencies [6]. However, the following disadvantages of this approach must be noted:

- Not all properties and characteristics can be scaled, e.g. material parameters, or some physical dimensions, e.g. mesh density and thickness, thin films, coatings, etc.

Thus, an approximation is introduced with an accuracy that is difficult to estimate.

- Manufacturing an exact scaled model of the feed array may represent a significant challenge, since even small deviations in the physical dimensions and/or electrical properties of the materials may result in unacceptable difference in RF characteristics.
- Not the actual reflector antenna, but another (scaled) antenna is characterized and the obtained characteristics would provide the knowledge about the antenna concept and geometry, but not the actual antenna.

In view of the above disadvantages, the measurement of the scaled model of the SAR antenna is considered as extremely technically challenging as well as not providing all necessary information and thus not satisfying the test requirements.

The third approach is the measurement of the feed array radiation followed by the calculation of the pattern of the entire antenna. In this approach, the feed array with the necessary part of its support structure and the satellite are characterized separately by measurements, while the pattern and gain of the entire SAR antenna, possibly including feed support and satellite structure, are calculated by a suitable electromagnetic computational tool.

This approach has several advantages but also some disadvantages. The main advantage is, clearly, that the verification measurements are done on a much smaller antenna under test, the feed array, which can be accurately characterized by an appropriate measurement technique. Another advantage, relevant for the BIOMASS configuration in particular, is that the reflector has an electrical size of about 17 wavelengths, which allows it to be accurately simulated with the rigorous Method of Moments (MoM) approach, including also the satellite, if proven necessary; thus, computational uncertainty is kept at a minimum.

The main disadvantage of this approach is that the number of uncertainty factors to be taken into account increases and the final uncertainty budget must include, in addition to the feed measurement uncertainty, several terms related to the accuracy of the model used in the calculations, as shown in Sect. 3, each of which must be carefully estimated. Another disadvantage is that the reflector shape and electrical properties must be accurately known for its proper modeling.

This approach has been applied previously and validated on a number of satellite reflector antennas, both commercial and scientific, such as Planck [7]. However, in view of the stringent accuracy requirements, it was not immediately clear if these requirements could be satisfied with this approach taking into account the specific features of the BIOMASS payload: low frequency, large size, accuracy of the reflector surface, etc. This approach was found to be the most promising one and it was investigated further, both by simulations and by measurements.

3 Uncertainty budget

The total uncertainty budget for the selected validation approach consists of the following terms:

(1) Measurement uncertainty of the feed
(2) Multiple interactions between the reflector and the satellite
(3) Influence of the reflector support arm
(4) Uncertainty of the field incident on the reflector, depending on the feed model used in the measurements
(5) Uncertainty of the reflector surface modeling
(6) Uncertainty of the simulation method
(7) Uncertainty related to deployment accuracy and repeatability
(8) Environmental phenomena, settling due to launch loads, aging over the mission life

In item 1, the uncertainty of the feed radiation pattern is taken into account depending on the chosen measurement technique. This uncertainty is obtained by estimating the influence of different factors specific for the chosen technique.

Items 2 and 3 describe the uncertainties in the field incident on the reflector due to multiple interactions between the feed array, satellite body, reflector support arm, and the reflector. During the measurements of the feed, either alone or with the satellite (or its model), these multiple interactions are not taken into account thus introducing an uncertainty described in the item 2. Similarly, the reflector support arm, and thus its scattering, is not present, which is described by the item 3. However, it can be investigated if the reflector support arm and satellite structure have a significant influence on the pattern, in which case these can be included in the modeling.

For the BIOMASS case, the feed sub-system is located on top of the rather large conductive satellite scattering the field, which may have a significant influence on the feed radiation pattern. One of the tasks is then to determine, if this scattering is significant, and thus the satellite, or part of it, must be included when measuring the feed characteristics for achieving the necessary accuracy for the entire antenna pattern. In item 4, several feed measurement configurations were considered: Configuration 1 is the feed array alone, attached to the test support structure; Configuration 2 further includes the triangular support structure used on the satellite and the top plate of the satellite, and Configuration 3 further includes the entire satellite structure. The considered feed measurement configurations 1, 2,

and 3 are illustrated in Fig. 2. Clearly, Configuration 1 is the simplest from the viewpoint of measurements, but it provides the least accurate feed model, since, e.g. scattering from the triangular support structure and the satellite is not taken into account. Configuration 3 is the most accurate in terms of the feed modeling, but it is also the most challenging for obtaining accurate measurement results due to much larger overall size of the object under test.

In item 5, the difference of the actual reflector from the one assumed during calculations is taken into account, including both the available knowledge of the physical surface properties and shape, and its representation in the simulation tool. Deployable reflector surface errors have contributions such as manufacturing accuracy, faceting error, and pillowing error. Their effects are rather different and their accurate modeling can be very complicated. Furthermore, for the mesh reflector the uncertainty of the (known) surface reflection coefficient should be taken into account. For the considered case of the BIOMASS deployable reflector, it was considered that it has a parabolic shape with known RMS deviation and correlation distance, and known surface reflection coefficient.

Item 6 takes into account the uncertainty of the simulation tool itself. For example, for electrically large reflectors, Physical Optics and Physical Theory of Diffraction approximations can be used to speed up the simulations with some compromise on the pattern accuracy.

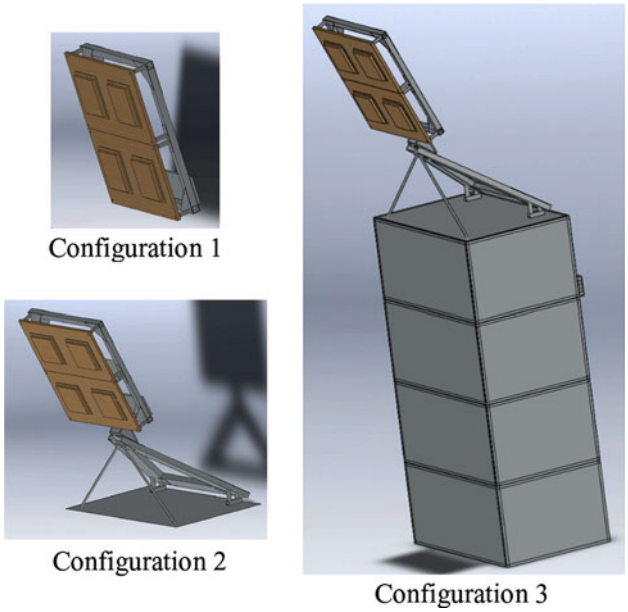

Fig. 2 BIOMASS feed measurement configurations. Configuration 1 consists of the 2 × 2 patch array and the test support structure. Configuration 2 further includes the triangular support structure and the satellite top plate. Configuration 3 further includes the rest of the satellite structure

The uncertainties mentioned in items 7 and 8 are not directly related to the verification methodology, but must also be included, since these represent additional uncertainty sources with the direct influence on the in-orbit SAR pattern uncertainty.

Investigations for the items 2–7 in the budget were carried out by simulations [4]. Item 8 can also be estimated by simulations from the available information, though it was not considered in this particular project. For the items 1 and 4, representative measurement data and typical uncertainties at 435 MHz were obtained from two measurement campaigns carried out with the prototype feed array [8] and a representative satellite model [9].

4 Simulations

A series of computer simulations were performed to investigate the above uncertainties; to this end, an accurate reference radiation pattern was established. This reference pattern does not need to represent the actual satellite and the antenna to all and smallest details, but it must be a sufficiently representative pattern that includes the effects of significant parts of the satellite. For example, the feed, the antenna, and the satellite should have the correct geometry and dimensions, elements of the feed array should have proper excitations, the feed and the reflector support structures should be representative, etc.

An accurate radiation pattern from the complete antenna, including the feed system, the feed support structure, the satellite body and the reflector with the support arm, was calculated with the GRASP software [10] based on the MoM approach (see Fig. 3a). The feed model included accurate representation of the patches on the ground plane and their proper excitation coefficients provided by the feed network (see Fig. 3b). The obtained radiation pattern was then used as a reference in the following comparisons.

The feed is a dual-polarized 2 × 2 patch array with a feed network providing specific excitations coefficients to compensate for the high cross-polar pattern of the offset

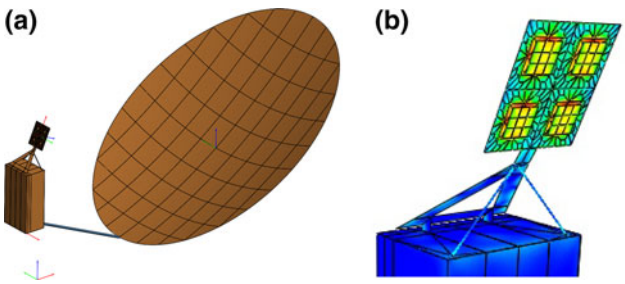

Fig. 3 GRASP model of the entire SAR antenna (**a**) and the simulated surface currents on the feed (**b**)

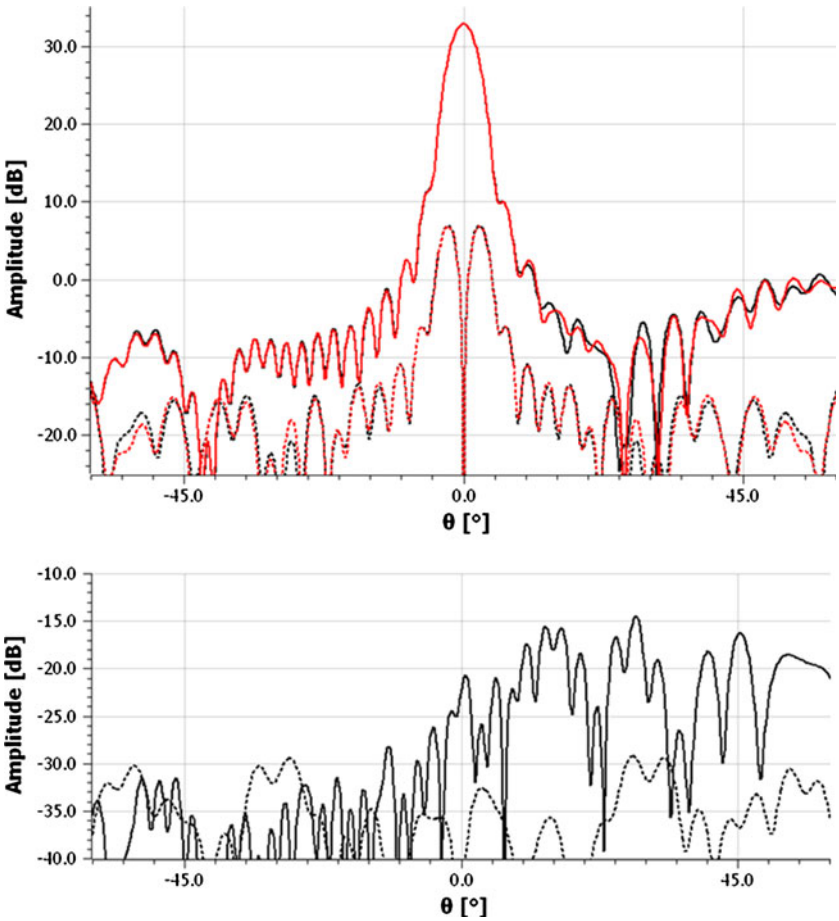

Fig. 4 Comparison between the reference pattern and the pattern calculated without the reflector support arm: solid lines are the co-polar components in the $\varphi = 0°$ (*offset*) plane and dashed lines are the cross-polar components in the $\varphi = 90°$ (*symmetry*) plane; pattern comparison (*top*) and pattern difference (*bottom*)

Table 1 Uncertainty budget for the peak directivity

Uncertainty item	SD σ, dB
1. Feed measurement uncertainty (neglecting measurement support frame)	0.03
2. Reflector-spacecraft interactions	0.01
3. Reflector support arm influence	0.01
4. Feed modeling (Conf. 2)	0.04
5. Reflector surface modeling	0.04
6. Numerical tool	0.01
7. Deployment accuracy	0.03
Root sum square	0.07

reflector antenna with a short focal distance [8]. The two feed ports designated H and V correspond to the polarization of the field incident of the reflector: the H-port provides the field polarized parallel to the horizontal plane, i.e. symmetry plane of the reflector, while the V-port provides the field polarized parallel to the vertical plane, i.e. the offset plane of the reflector. The entire antenna coordinate system, *xyz*, is defined such that the *xz*-plane is the offset plane of the reflector and the *yz*-plane is the symmetry plane of the reflector with *z*-axis coinciding with the pattern peak, see Fig. 3a.

The feed measurements were simulated by calculating the pattern from the feed as if it was measured in a radio anechoic chamber. Different measurement configurations were then considered corresponding to the items in the uncertainty budget. The simulated feed pattern is then represented in terms of spherical wave expansion.

For the investigation of item 2, a simplified problem was considered, where only the incident field was used to illuminate the reflector and the secondary field was calculated and compared with the reference. In this simplified problem, the multiple scattering between the reflector and the feed (in Configuration 3: the feed array, its support structure, and the entire satellite) was thus not taken into account. The secondary field from this simplified problem was then compared with the reference field and the uncertainty was estimated from the difference between the two patterns.

In a similar way, the simulation was carried out with and without presence of the reflector support arm (item 3 in the budget). Removing consecutively the satellite and the feed support structure, different feed configurations were simulated (item 4 in the budget), see Fig. 2. Uncertainties

related to the deployment accuracy, repeatability, and the reflector surface errors were simulated introducing assumed deviations in the reflector position and orientation and the reflector shape (items 5 and 7 in the budget).

An example of the pattern comparison and the pattern difference from the investigation of the budget item 3 is shown in Fig. 4. It was found that the difference between the patterns are mainly observed in the $\varphi = 0°$ plane (xz-plane) for the co-polar component and in the $\varphi = 90°$ plane (yz-plane) for the cross-polar component, and thus only these cuts are shown in Fig. 4.

It is seen from Fig. 4 that the effect of removing the reflector support arm is very small; only small difference is seen at very low levels of the co-polar pattern, while for the cross polar pattern the difference is almost negligible. The peaks of the co-polar pattern difference are at the level of about −48 dB from the pattern peak. An error signal at this level would cause maximum deviation of about ±0.035 dB around the pattern peak, which corresponds to a standard deviation of about 0.012 dB.

In this way, the uncertainty of the secondary antenna pattern for all items in the budget was evaluated; see the results in Table 1.

5 Measurement campaigns

To obtain realistic measurement uncertainty estimates and investigate possible problems related to characterization of the feed at P-band, two measurement campaigns were carried out [9]. The first campaign included measurements of the prototype feed array in all configurations, 1, 2, and 3, at the DTU-ESA Spherical Near-Field Antenna Test Facility at the Technical University of Denmark (DTU) [11]. The DTU-ESA Facility is an ESA external reference laboratory with primary focus on high-accuracy antenna measurements in the frequency range from 400 MHz to 40 GHz. The anechoic chamber of the DTU-ESA Facility has the dimensions of $18 \times 14 \times 12$ m^3; it is lined with 120 cm (48 inch) absorbers providing reflectivity level of about −35 dB at 400 MHz going down to −50 dB from 1 GHz up to 40 GHz. Antennas up to 6 m in diameter and up to 250 kg in weight can be measured. A collection of dual-polarized probes and Standard Gain Horns covers the complete 0.4–40 GHz frequency range.

The measurement of the feed array on top of the BIOMASS satellite model (Conf. 3) at the DTU-ESA Facility is shown in Fig. 5. The probe used in these measurements (seen at the right side in Fig. 5) is a wide-band open-boundary quad-ridge horn developed at DTU specifically for these low frequencies [12].

The second campaign included measurements of the feed array in configurations 1 and 2 at the Near-Field facility of the Naval Maintenance Establishment (NME) in Den Helder, the Netherlands, with Planar Near-Field (PNF) and Cylindrical Near-Field (CNF) techniques [9]. The measurement of the feed array in Configuration 1 at the NME Facility is shown in Fig. 6.

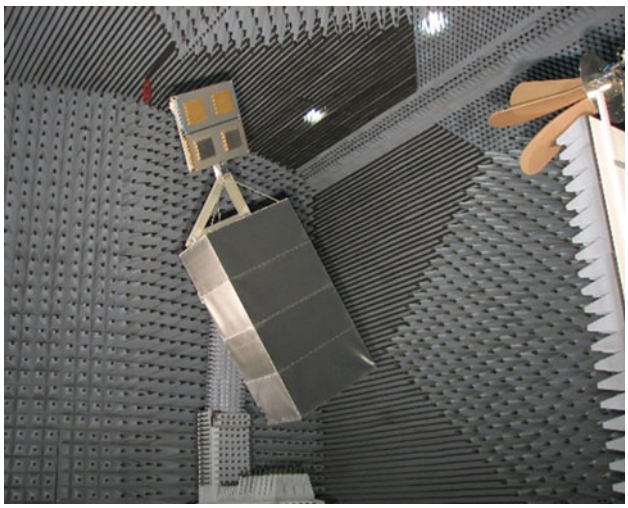

Fig. 5 Measurement of the feed array on top of the BIOMASS satellite model (Conf. 3) at the DTU-ESA Facility

In the SNF technique, first, two orthogonal components of the near field of the Antenna Under Test (AUT) are measured by a dual-polarized probe at a number of points on a full sphere around the AUT. Next, the near field is transformed to the corresponding far field using a mathematical algorithm based on a spherical wave expansion of the near field, properly taking into account characteristics of the probe [13].

In the PNF and CNF techniques, similar to the SNF technique, the AUT near-field is measured at a number of points on a planar surface in front of the AUT or cylindrical surface surrounding the AUT, respectively. The near-to-far-field transformation is then based, respectively, on a plane wave expansion and a cylindrical wave expansion [14, 15].

The main advantage of the PNF technique is that the AUT is held fixed, while the probe is systematically moved on a plane in front of it. On the other hand, the PNF technique is only suitable for highly directive antennas, since the field outside the scanned plane is ignored. The calculated far-field pattern is valid in a limited angular region typically not exceeding about ±60° in the main planes or even less. The CNF technique has the advantage of covering complete circle in one plane, but has a similar limited angular range in the other plane, while the SNF technique provides the full-sphere coverage. In both of these techniques, in the standard setups, the AUT is rotated either around one axis, in the CNF technique, or around two orthogonal axes, in the SNF technique. There exist also such SNF setups, where the AUT is rotated around one

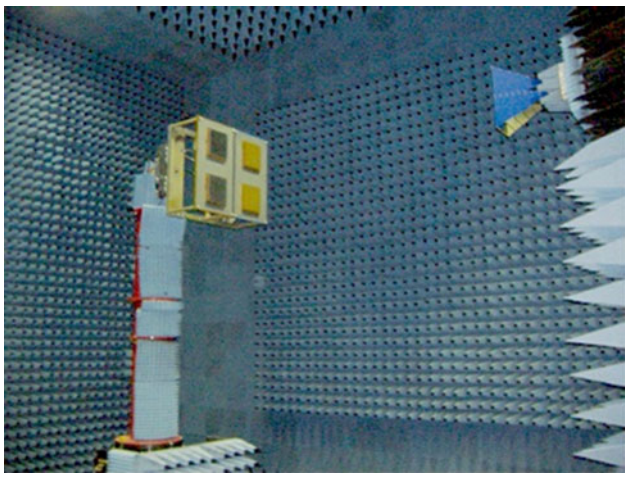

Fig. 6 Measurement of the feed array (Conf. 1) at the Naval Maintenance Establishment (with permission from [9])

vertical axis, while the probe is moved on a circular arch thus providing partial-sphere coverage around the AUT.

In each measurement campaign, special attention was given to investigation of the measurement uncertainty. In particular, the uncertainty items known to give the largest contributions at these low frequencies were estimated by performing additional measurements: multiple reflections between the AUT and probe, scattering from the chamber walls, and scattering from the AUT positioner. In addition, the effect of the test support frame interfacing the AUT and the antenna positioner mounting flange was investigated.

The comparison of the measurement results from the campaigns have shown that the SNF technique provided the results with the smallest uncertainty as well as the full-sphere coverage for the measured data, and this technique was recommended for the on-ground performance verification of the feed array. Several recommendations were also given regarding improvements of the test procedures to reduce critical uncertainty sources in the gain measurement.

6 Simulations using the measured feed data

The measurement campaigns have provided the necessary feed radiation patterns with realistic uncertainties for all considered configurations. Several additional measurements carried out for the measurement uncertainty investigation allowed separating the individual uncertainties and creating additional results with and without these uncertainties.

The measurement data were then used in calculation of the secondary pattern. Comparing the secondary patterns calculated with different input measurement data (i.e. with and without particular uncertainty) provided estimates for the so-called propagation coefficients for those uncertainties into the secondary pattern. These propagation coefficients quantify the influence of particular feed measurement uncertainty sources on the secondary pattern. A coefficient <1 means that the uncertainty source has less influence on the secondary pattern than on the feed pattern.

It was found that most of the measurement uncertainties have propagation coefficients significantly <1 and their contribution to the secondary pattern is very small. On the other hand, it was found that the effect of the test support frame, interfacing the feed and the antenna positioner, has propagation coefficient close to 1, thus directly contributing to the uncertainty of the secondary pattern.

It was also found that the effect of the test support frame is the largest term in the feed uncertainty budget, exceeding the other terms by at least a factor of two. This large effect is explained by several factors: non-optimum design of the frame, its proximity to the edges of the feed array carrying rather strong currents, as well as possible scattering of the back-radiated fields. As an outcome, recommendations were given regarding development of a special design of this support frame and modification of the feed array design, if possible, to decrease its back radiation, thus ensuring their minimum interference during the on-ground performance verification.

7 Analysis of the results

Summarizing the results of all the investigations, the following conclusions have been reached (see Table 1):

- The impact of the satellite body on the secondary pattern of the reflector illuminated by the feed is negligible for the specific BIOMASS satellite configuration
- The impact of the reflector support arm on the secondary pattern is negligible for this specific configuration
- The calculation uncertainty of the employed numerical tool, GRASP software based on the MoM approach, is negligible. Application of the combined Physical Optics and Physical Theory of Diffraction approach was also investigated and found possible
- Sensitivity analysis regarding relative pointing and displacement of the feed and reflector has concluded that all displacement and pointing uncertainties that keep the beam maximum within 0.05° from the nominal direction will not affect the pattern shape, only the pointing direction
- Sensitivity analysis regarding the reflector surface shape has concluded that for a typical value of 5 mm RMS for the reflector surface uncertainty, it is recommended to keep the correlation distance below 2.5 m

- The analysis of the simulation results for the three feed measurement configurations has concluded that Conf. 1 does not provide enough accuracy to meet the pattern uncertainty and pointing requirements, while both Conf. 2 and Conf. 3 provide sufficient accuracy of the incident field
- The analysis of the measurement uncertainties for the three feed configurations has shown that Conf. 3 does not meet the secondary pattern uncertainty requirements, while both Conf. 1 and Conf. 2 have an acceptably low uncertainty.

Summarizing the above conclusions, the most promising approach consists of measurement of the radiation characteristics of the feed with its triangular support structure and the satellite top plate (Conf. 2) with the SNF technique, followed by calculation of the pattern and gain of the entire SAR antenna by the MoM computational tool of GRASP, or similar accurate simulation software.

In the proposed performance validation methodology, the gain of the antenna is represented by a product of the directivity and the radiation efficiency, where the latter consists of two contributions: measured feed radiation efficiency and calculated reflector radiation efficiency. The feed radiation efficiency is determined from the SNF measurements by comparing the total radiated power of the feed and that of the standard gain horn (SGH) antenna. Thus, the total uncertainty budget for the gain consists of several terms with the largest contributions from the reflector antenna peak directivity uncertainty, feed total radiated power, and SGH uncertainty.

The final uncertainty budgets for the secondary pattern directivity and gain compiled using the results of the above simulations and the available measurements are shown in Table 1 and Table 2, respectively. It is noted that the obtained estimate for the gain (0.16 dB) is close, but slightly exceeding the specified requirement (0.15 dB). Several improvements of the measurement procedures are recommended to be implemented to decrease the largest terms in the gain uncertainty budget: employing a SGH with smaller calibration uncertainty and applying compensation for the largest uncertainties in the feed measurement, e.g. stray signal suppression, drift correction, etc.

Table 2 Uncertainty budget for the peak gain

Uncertainty item	SD σ, dB
1. SAR antenna peak directivity	0.07
2. Feed total radiated power	0.09
3. SGH radiation efficiency	0.10
4. Feed mismatch correction	0.01
5. SGH mismatch correction	0.01
6. Signal source mismatch	0.04
7. Drift	0.03
8. Cable variations	0.02
9. Reflector radiation efficiency[a]	–
Root sum square	0.16

[a] The calculation uncertainty of the reflector mesh radiation efficiency is assumed to be negligibly small in view of negligibly small conductivity loss of the mesh at 435 MHz

8 Proposed performance verification methodology—step by step

The proposed performance verification methodology for the P-band SAR payload for the BIOMASS candidate mission is the following:

Measurements:

(1) The S-parameters of the feed in Conf. 2 are measured
(2) The full-sphere complex relative pattern of the feed in Conf. 2 is measured with the SNF technique
(3) The radiation efficiency of the feed in Conf. 2 is measured using the substitution technique with a calibrated gain standard
(4) Measurements for establishing uncertainty budgets for the radiation pattern and efficiency are carried out
(5) Post-processing of the measured data is carried out, including transformation from the measurement to the feed coordinate system, conversion to the necessary time convention, normalization, and data format.

Simulations:

(1) The spherical wave expansion (SWE) of the feed is calculated
(2) The reflector model is established and the scattered field is calculated using the feed SWE as incident field. Radiation efficiency of the reflector is calculated
(3) Total secondary field is calculated from the sum of the incident and scattered fields. Directivity of the secondary pattern is calculated
(4) Gain is calculated by a product of the secondary pattern directivity, feed radiation efficiency, and reflector radiation efficiency
(5) Transformation to the necessary output coordinate system, conversion to the necessary time convention, normalization, and data format
(6) Calculations for establishing uncertainty budgets for the radiation pattern and gain are carried out.

Further details of the proposed methodology can be found in [4].

An independent in-orbit validation of the BIOMASS SAR pattern characteristics, checking also for geometrical and deployment errors beyond the accuracies assumed for

the uncertainty budget, will finally be made as part of the commissioning phase of the mission.

9 Conclusions

An optimum electrical performance verification methodology is proposed for very large deployable and fixed reflector antennas not suitable for traditional measurements of radiation characteristics of the entire antenna. The methodology was developed for the BIOMASS P-band SAR antenna as part of its on-ground performance verification, but it can also be applied to other mechanically or electrically very large reflector antennas.

The two-step methodology is based on accurate measurements of the feed characteristics, such as the complex pattern and the radiation efficiency, and then calculation of the radiation pattern and gain of the entire antenna with an accurate computational software. One critical feature of the proposed methodology is determination of the necessary part of the feed support structure to be included in characterization by the measurements and the necessary parts of the reflector antenna, e.g. its support structure, a part or an entire satellite, to be included in the calculation of the secondary pattern. Another critical feature is the availability of accurate knowledge of the reflector geometry and the electrical characteristics of the reflecting surface.

For the BIOMASS P-band SAR payload, the compliance analysis of the derived uncertainty budgets for the main parameters was carried out and it was shown that the proposed methodology allows achieving the specified requirements for all characteristics. Several recommendations on improvement of the test procedures to reduce the largest uncertainty sources were provided. In particular, it was found critical to develop a suitable design of the test support frame for the feed, which introduces minimum disturbance into the measured feed pattern. Modifications of the feed array design to decrease its back radiation were also recommended, thus ensuring minimum interference between the feed and the test support frame during the feed characterization.

Acknowledgments This work was supported by European Space Agency under the contract No. 4000102325/10/NL/JA "Study of Very Large Aperture P-Band Antenna Performance Verification Methodology and Facilities—BIOMASS", with a funding through the Instrument Pre-development line of the Earth Observation Envelop Programme.

References

1. Imbriale, W.A., Gao, S., Boccia, L.: Space antenna handbook. John Wiley and Sons Ltd, Bristol (2012)
2. ESA: The Living Planet Programme—Earth Explorers. Available from http://www.esa.int/Our_Activities/Observing_the_Earth/The_Living_Planet_Programme/Earth_Explorers
3. R. Mizzoni, G. Orlando, P. Valle: Unfurlable reflector SAR antenna at P-band. In: Proceedings of EuCAP 2009, Berlin, Germany
4. S. Pivnenko, O.S. Kim, and O. Breinbjerg: Study of very large aperture P-band antenna performance verification methodology and facilities. Summary Report. ESTEC contract No. 4000102325/10/NL/JA Tech. University of Denmark, Deparment of Electrical Engineering, R758, (2012)
5. S. Pivnenko, O.S. Kim, O. Breinbjerg, K. Pontoppidan, A. Østergaard, and C. C. Lin: Electrical performance verification methodology for the P-band SAR payload of the BIOMASS candidate mission. In: Proceedings of 34th ESA Antenna Workshop, Noordwijk, The Netherlands (2012)
6. IEEE Standard Test Procedures for Antennas, IEEE Std 149-1979
7. J. Tauber et al.: Planck pre-launch status: the optical system. Astronomy and astrophysics (2009)
8. P. Valle, G. Orlando, R. Mizzoni, F. Heliere, K. van't Klooster: P-Band feedarray for BIOMASS, In: Proceedings of EuCAP 2012, Prague, Czech Republic
9. S. Pivnenko et al: Measurement campaigns for selection of optimum on-ground performance verification approach for large deployable reflector antenna. In: Proceedings of 34th Annual AMTA Meeting and Symp., Bellevue, WA, USA (2012)
10. GRASP software: http://www.ticra.com
11. DTU-ESA Spherical Near-Field Antenna Test Facility. Available online from: http://www.dtu.dk/centre/ems/English/research/dtu_esa_facility.aspx
12. O.S. Kim, S. Pivnenko, and O. Breinbjerg: 0.4–1.2 GHz hybrid Al-CFRP open-boundary quad-ridge horn. In: Proceedings of 33rd ESA Antenna Workshop on Challenges for Space Antenna Systems, Noordwijk, The Netherlands (2011)
13. J. E. Hansen (Ed.), Spherical near-field antenna measurements. Peter Peregrinus Ltd., London, UK (1988)
14. Yaghjian, A.D.: An overview of near-field antenna measurements. IEEE Trans. Antennas Propagat. **34**(1), 30–45 (1986)
15. C.A. Balanis (Ed.), Modern Antenna Handbook. Ch. 19: near-field scanning measurements: theory and practice by M.H. Francis and R.C. Wittmann, John Wiley and Sons, Ltd (2008)